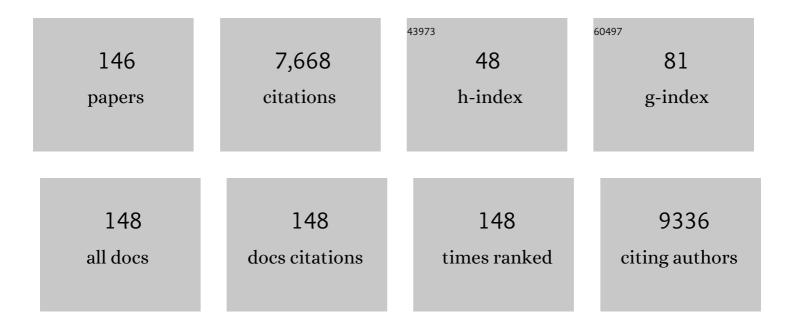
## Xiurong Yang

List of Publications by Year in descending order

Source: https://exaly.com/author-pdf/3012464/publications.pdf Version: 2024-02-01



XILIPONC YANC

#	Article	IF	CITATIONS
1	Fluorescence immunoassay based on alkaline phosphatase-induced in situ generation of fluorescent non-conjugated polymer dots. Chinese Chemical Letters, 2023, 34, 107672.	4.8	4
2	Zeolitic imidazolate framework-67 accelerates infected diabetic chronic wound healing. Chemical Engineering Journal, 2022, 430, 133091.	6.6	22
3	A dual-amplification mode and Cu-based metal-organic frameworks mediated electrochemical biosensor for sensitive detection of microRNA. Biosensors and Bioelectronics, 2022, 202, 113992.	5.3	32
4	Study on Synthesis and Antibacterial Properties of AgNPs@ZIF-67 Composite Nanoparticles <sup>※</sup> . Acta Chimica Sinica, 2022, 80, 110.	0.5	1
5	Tuning Phase Structure of Nickel–Ruthenium Alloys via MOFs In Situ Hydrolysis toward Enhanced Hydrogen Evolution Performance in Alkaline. Small Methods, 2022, 6, e2101188.	4.6	13
6	Modulating the Electronic Structure by Ruthenium Doping Endows Cobalt Phosphide Nanowires with Enhanced Alkaline Hydrogen Evolution Activity. ACS Applied Energy Materials, 2022, 5, 697-704.	2.5	13
7	An electrochemical sensor for sensitive detection of dopamine based on a COF/Pt/MWCNT–COOH nanocomposite. Chemical Communications, 2022, 58, 6092-6095.	2.2	46
8	A fluorescence turn-on biosensor utilizing silicon-containing nanoparticles: Ultra-sensitive sensing for α-glucosidase activity and screening for its potential inhibitors. Biosensors and Bioelectronics, 2022, 214, 114504.	5.3	17
9	A thiamine-triggered fluormetric assay for acetylcholinesterase activity and inhibitor screening based on oxidase-like activity of MnO2 nanosheets. Talanta, 2021, 221, 121362.	2.9	27
10	Holey nitrogen-doped graphene aerogel for simultaneously electrochemical determination of ascorbic acid, dopamine and uric acid. Talanta, 2021, 224, 121851.	2.9	67
11	Sensitive and Programmable "Signal-Off―Electrochemiluminescence Sensing Platform Based on Cascade Amplification and Multiple Quenching Mechanisms. Analytical Chemistry, 2021, 93, 2644-2651.	3.2	30
12	Electrochemistry and Electrochemiluminescence of Coumarin Derivative Microrods: Mechanism Insights. Analytical Chemistry, 2021, 93, 3461-3469.	3.2	20
13	A ratiometric electrochemiluminescence strategy based on two-dimensional nanomaterial-nucleic acid interactions for biosensing and logic gates operation. Biosensors and Bioelectronics, 2021, 178, 113022.	5.3	23
14	Electrochemically induced in-situ surface self-reconstruction on Ni, Fe, Zn ternary-metal hydroxides towards the oxygen-evolution performance. Chemical Engineering Journal, 2021, 410, 128331.	6.6	22
15	DNA Assemblyâ€Based Stimuliâ€Responsive Systems. Advanced Science, 2021, 8, 2100328.	5.6	44
16	Label-Free and Sensitive Electrochemical Biosensor for Amplification Detection of Target Nucleic Acids Based on Transduction Hairpins and Three-Leg DNAzyme Walkers. Analytical Chemistry, 2021, 93, 8962-8970.	3.2	29
17	Rational Construction of Rutheniumâ€Cobalt Oxides Heterostructure in ZIFsâ€Derived Doubleâ€Shelled Hollow Polyhedrons for Efficient Hydrogen Evolution Reaction. Small, 2021, 17, e2100998.	5.2	27
18	Electrochemiluminescence Biosensor Based on Entropy-Driven Amplification and a Tetrahedral DNA Nanostructure for miRNA-133a Detection. Analytical Chemistry, 2021, 93, 11809-11815.	3.2	61

#	Article	IF	CITATIONS
19	An intensive and glow-type chemiluminescence of luminol-embedded, guanosine-derived hydrogel. Talanta, 2021, 230, 122351.	2.9	16
20	Electrochemical-Based DNA Logic Devices Regulated by the Diffusion and Intercalation of Electroactive Dyes. ACS Applied Materials & amp; Interfaces, 2021, 13, 42250-42257.	4.0	14
21	Electrochemical Immunosensor for Cardiac Troponin I Detection Based on Covalent Organic Framework and Enzyme-Catalyzed Signal Amplification. Analytical Chemistry, 2021, 93, 13572-13579.	3.2	68
22	Label-free immunosensor for cardiac troponin I detection based on aggregation-induced electrochemiluminescence of a distyrylarylene derivative. Biosensors and Bioelectronics, 2021, 192, 113532.	5.3	20
23	Contrary Logic Pair Library, Parity Generator/Checker and Various Concatenated Logic Circuits Engineered by a Labelâ€Free and Immobilizationâ€Free Electrochemiluminescence Resonance Energy Transfer System. Small, 2021, 17, e2102881.	5.2	20
24	Real-Time Analysis of Specific Binding between Apolipoprotein E Isoforms and Amyloid β-Peptide by Dual Polarization Interferometry. Analytical Chemistry, 2021, 93, 1472-1479.	3.2	6
25	Cu2+ enhanced chemiluminescence of carbon dots-H2O2 system in alkaline solution. Talanta, 2020, 208, 120380.	2.9	16
26	Au and Au-Based nanomaterials: Synthesis and recent progress in electrochemical sensor applications. Talanta, 2020, 206, 120210.	2.9	213
27	Electrospun Ru–RuO <sub>2</sub> /MoO <sub>3</sub> carbon nanorods with multi-active components: a Pt-like catalyst for the hydrogen evolution reaction. Chemical Communications, 2020, 56, 739-742.	2.2	38
28	Enzyme-induced in situ generation of polymer carbon dots for fluorescence immunoassay. Sensors and Actuators B: Chemical, 2020, 306, 127583.	4.0	41
29	Dual-Readout Tyrosinase Activity Assay Facilitated by a Chromo-Fluorogenic Reaction between Catechols and Naphthoresorcin. Analytical Chemistry, 2020, 92, 2316-2322.	3.2	27
30	A pH-regulated stimuli-responsive strategy for RNA-cleaving DNAzyme. Science China Chemistry, 2020, 63, 404-410.	4.2	5
31	Superb Hydrogen Evolution by a Pt Nanoparticle-Decorated Ni <sub>3</sub> S <sub>2</sub> Microrod Array. ACS Applied Materials & Interfaces, 2020, 12, 39163-39169.	4.0	41
32	Ru nanoparticles encapsulated in ZIFs-derived porous N-doped hierarchical carbon nanofibers for enhanced hydrogen evolution reaction. Catalysis Science and Technology, 2020, 10, 7302-7308.	2.1	13
33	Ratiometric Electrochemiluminescent/Electrochemical Strategy for Sensitive Detection of MicroRNA Based on Duplex-Specific Nuclease and Multilayer Circuit of Catalytic Hairpin Assembly. Analytical Chemistry, 2020, 92, 8614-8622.	3.2	70
34	In situ formation of fluorescent silicon-containing polymer dots for alkaline phosphatase activity detection and immunoassay. Science China Chemistry, 2020, 63, 554-560.	4.2	22
35	Novel electrochemiluminescence solid-state pH sensor based on an i-motif forming sequence and rolling circle amplification. Chemical Communications, 2020, 56, 8786-8789.	2.2	7
36	Label-Free and Regenerable Aptasensor for Real-Time Detection of Cadmium(II) by Dual Polarization Interferometry. Analytical Chemistry, 2020, 92, 10007-10015.	3.2	40

#	Article	IF	CITATIONS
37	Self-Enhanced Chemiluminescence of Tris(bipyridine) Ruthenium(II) Derivative Nanohybrids: Mechanism Insight and Application for Sensitive Silver Ions Detection. Analytical Chemistry, 2020, 92, 7265-7272.	3.2	27
38	Identifying the Activation Mechanism and Boosting Electrocatalytic Activity of Layered Perovskite Ruthenate. Small, 2020, 16, e1906380.	5.2	13
39	Electrochemiluminescence Immunosensor Based on Au Nanocluster and Hybridization Chain Reaction Signal Amplification for Ultrasensitive Detection of Cardiac Troponin I. ACS Sensors, 2019, 4, 2778-2785.	4.0	48
40	Atomic and electronic modulation of self-supported nickel-vanadium layered double hydroxide to accelerate water splitting kinetics. Nature Communications, 2019, 10, 3899.	5.8	355
41	Dual amplification ratiometric biosensor based on a DNA tetrahedron nanostructure and hybridization chain reaction for the ultrasensitive detection of microRNA-133a. Chemical Communications, 2019, 55, 11551-11554.	2.2	50
42	Highly Luminescent and Self-Enhanced Electrochemiluminescence of Tris(bipyridine) Ruthenium(II) Nanohybrid and Its Sensing Application for Label-Free Detection of MicroRNA. Analytical Chemistry, 2019, 91, 13237-13243.	3.2	47
43	A duplex connection can further illuminate G-quadruplex/crystal violet complex. Chemical Communications, 2019, 55, 1911-1914.	2.2	17
44	Fluorescence Immunoassay Based on the Alkaline Phosphatase Triggered in Situ Fluorogenic Reaction of <i>o</i> -Phenylenediamine and Ascorbic Acid. Analytical Chemistry, 2019, 91, 2978-2984.	3.2	99
45	Fluorometric and Colorimetric Dual-Readout Immunoassay Based on an Alkaline Phosphatase-Triggered Reaction. Analytical Chemistry, 2019, 91, 7828-7834.	3.2	60
46	Ultrasensitive Immunosensor for Cardiac Troponin I Detection Based on the Electrochemiluminescence of 2D Ru-MOF Nanosheets. Analytical Chemistry, 2019, 91, 10156-10163.	3.2	108
47	A Ratiometric Fluorescent DNA Radar Based on Contrary Response of DNA/Silver Nanoclusters and G-Quadruplex/Crystal Violet. ACS Applied Materials & Interfaces, 2019, 11, 25066-25073.	4.0	31
48	Label-free Pb2+ detection on the layer-by-layer platform using real-time dual polarization interferometry. Talanta, 2019, 202, 336-341.	2.9	9
49	Establishment of Logic Gates Based on Conformational Changes in a Multiple-Factor Biomolecule Interaction Process by Dual Polarization Interferometry. Analytical Chemistry, 2019, 91, 6971-6975.	3.2	8
50	Ni <sub>17</sub> W <sub>3</sub> Nanoparticles Decorated WO <sub>2</sub> Nanohybrid Electrocatalyst for Highly Efficient Hydrogen Evolution Reaction. ACS Applied Energy Materials, 2019, 2, 2409-2413.	2.5	30
51	Single-atom ruthenium based catalyst for enhanced hydrogen evolution. Applied Catalysis B: Environmental, 2019, 249, 91-97.	10.8	146
52	A wavelength-resolved electrochemiluminescence resonance energy transfer ratiometric immunosensor for detection of cardiac troponin I. Analyst, The, 2019, 144, 6554-6560.	1.7	13
53	Dual-Wavelength Ratiometric Electrochemiluminescence Immunosensor for Cardiac Troponin I Detection. Analytical Chemistry, 2019, 91, 1524-1531.	3.2	105
54	An electric potential modulated cascade of catalyzed hairpin assembly and rolling chain amplification for microRNA detection. Biosensors and Bioelectronics, 2019, 126, 565-571.	5.3	46

#	Article	IF	CITATIONS
55	Alkaline Phosphatase Assay Based on the Chromogenic Interaction of Diethanolamine with 4-Aminophenol. Analytical Chemistry, 2018, 90, 6339-6345.	3.2	62
56	Construction of amorphous interface in an interwoven NiS/NiS <sub>2</sub> structure for enhanced overall water splitting. Journal of Materials Chemistry A, 2018, 6, 8233-8237.	5.2	159
57	Cobalt Sulfide Nanowires Core Encapsulated by a N, S Codoped Graphitic Carbon Shell for Efficient Oxygen Reduction Reaction. Small, 2018, 14, e1703642.	5.2	75
58	A pH-controlled bidirectionally pure DNA hydrogel: reversible self-assembly and fluorescence monitoring. Chemical Communications, 2018, 54, 4621-4624.	2.2	38
59	FRET Effect between Fluorescent Polydopamine Nanoparticles and MnO <sub>2</sub> Nanosheets and Its Application for Sensitive Sensing of Alkaline Phosphatase. ACS Applied Materials & Interfaces, 2018, 10, 6560-6569.	4.0	175
60	Fluorescence Immunoassay Based on the Phosphate-Triggered Fluorescence Turn-on Detection of Alkaline Phosphatase. Analytical Chemistry, 2018, 90, 3505-3511.	3.2	145
61	Photo-Induced Electron Transfer-Based Versatile Platform with G-Quadruplex/Hemin Complex as Quencher for Construction of DNA Logic Circuits. Analytical Chemistry, 2018, 90, 3437-3442.	3.2	42
62	Inner Filter Effect-Based Sensor for Horseradish Peroxidase and Its Application to Fluorescence Immunoassay. ACS Sensors, 2018, 3, 183-190.	4.0	67
63	A luminescent europium-dipicolinic acid nanohybrid for the rapid and selective sensing of pyrophosphate and alkaline phosphatase activity. Nanoscale, 2018, 10, 7163-7170.	2.8	41
64	Copper sulfide nanoplates as nanosensors for fast, sensitive and selective detection of DNA. Talanta, 2018, 178, 905-909.	2.9	12
65	When NiO@Ni Meets WS <sub>2</sub> Nanosheet Array: A Highly Efficient and Ultrastable Electrocatalyst for Overall Water Splitting. ACS Central Science, 2018, 4, 112-119.	5.3	120
66	One-pot synthesis of interconnected Pt95Co5 nanowires with enhanced electrocatalytic performance for methanol oxidation reaction. Nano Research, 2018, 11, 2562-2572.	5.8	56
67	Classical Triplex Molecular Beacons for MicroRNA-21 and Vascular Endothelial Growth Factor Detection. ACS Sensors, 2018, 3, 2438-2445.	4.0	25
68	Bio-inspired FeN <sub>5</sub> moieties anchored on a three-dimensional graphene aerogel to improve oxygen reduction catalytic performance. Journal of Materials Chemistry A, 2018, 6, 18488-18497.	5.2	53
69	Polymethyldopa Nanoparticles-Based Fluorescent Sensor for Detection of Tyrosinase Activity. ACS Sensors, 2018, 3, 1855-1862.	4.0	48
70	An Enzyme Cascade-Triggered Fluorogenic and Chromogenic Reaction Applied in Enzyme Activity Assay and Immunoassay. Analytical Chemistry, 2018, 90, 7754-7760.	3.2	60
71	<i>N</i> -(Aminobutyl)- <i>N</i> -(ethylisoluminol)-functionalized gold nanoparticles on cobalt disulfide nanowire hybrids for the non-enzymatic chemiluminescence detection of H <sub>2</sub> O <sub>2</sub> . Nanoscale, 2018, 10, 14847-14851.	2.8	26
72	Pt-like catalytic behavior of MoNi decorated CoMoO <sub>3</sub> cuboid arrays for the hydrogen evolution reaction. Journal of Materials Chemistry A, 2018, 6, 15558-15563.	5.2	39

#	Article	IF	CITATIONS
73	Polydopamine Nanoparticles as Efficient Scavengers for Reactive Oxygen Species in Periodontal Disease. ACS Nano, 2018, 12, 8882-8892.	7.3	401
74	Real-Time Analysis of Binding Events between Different Aβ <sub>1–42</sub> Species and Human Lilrb2 by Dual Polarization Interferometry. Analytical Chemistry, 2017, 89, 2606-2612.	3.2	21
75	Fine Co Nanoparticles Encapsulated in a N-Doped Porous Carbon Matrix with Superficial N-Doped Porous Carbon Nanofibers for Efficient Oxygen Reduction. ACS Applied Materials & Interfaces, 2017, 9, 21747-21755.	4.0	98
76	Experimental and theoretical insights into sustained water splitting with an electrodeposited nanoporous nickel hydroxide@nickel film as an electrocatalyst. Journal of Materials Chemistry A, 2017, 5, 7744-7748.	5.2	90
77	Ultra-Sensitive Colorimetric Assay System Based on the Hybridization Chain Reaction-Triggered Enzyme Cascade Amplification. ACS Applied Materials & Interfaces, 2017, 9, 167-175.	4.0	64
78	In Situ Fluorogenic and Chromogenic Reactions for the Sensitive Dual-Readout Assay of Tyrosinase Activity. Analytical Chemistry, 2017, 89, 10529-10536.	3.2	56
79	Ultrafine Pt Nanoparticle-Decorated Co(OH) <sub>2</sub> Nanosheet Arrays with Enhanced Catalytic Activity toward Hydrogen Evolution. ACS Catalysis, 2017, 7, 7131-7135.	5.5	195
80	Fluorescence Light-Up Biosensor for MicroRNA Based on the Distance-Dependent Photoinduced Electron Transfer. Analytical Chemistry, 2017, 89, 8429-8436.	3.2	79
81	Bromine and nitrogen co-doped tungsten nanoarrays to enable hydrogen evolution at all pH values. Journal of Materials Chemistry A, 2017, 5, 17856-17861.	5.2	10
82	Real-Time Study of the Interaction between G-Rich DNA Oligonucleotides and Lead Ion on DNA Tetrahedron-Functionalized Sensing Platform by Dual Polarization Interferometry. ACS Applied Materials & Interfaces, 2017, 9, 41568-41576.	4.0	19
83	Three-Dimensional Structures of MoS <sub>2</sub> @Ni Core/Shell Nanosheets Array toward Synergetic Electrocatalytic Water Splitting. ACS Applied Materials & Interfaces, 2016, 8, 14521-14526.	4.0	132
84	Carbon dots-assisted colorimetric and fluorometric dual-mode protocol for acetylcholinesterase activity and inhibitors screening based on the inner filter effect of silver nanoparticles. Analyst, The, 2016, 141, 3280-3288.	1.7	80
85	Colorimetric Logic Gate for Pyrophosphate and Pyrophosphatase via Regulating the Catalytic Capability of Horseradish Peroxidase. ACS Applied Materials & Interfaces, 2016, 8, 29529-29535.	4.0	44
86	Fluorescence Immunoassay System via Enzyme-Enabled in Situ Synthesis of Fluorescent Silicon Nanoparticles. Analytical Chemistry, 2016, 88, 9789-9795.	3.2	98
87	A fluorescent ELISA based on the enzyme-triggered synthesis of poly(thymine)-templated copper nanoparticles. Nanoscale, 2016, 8, 16846-16850.	2.8	41
88	A versatile strategy to fabricate MOFs/carbon material integrations and their derivatives for enhanced electrocatalysis. RSC Advances, 2016, 6, 7728-7735.	1.7	28
89	Enhanced Catalytic Activities of Surfactant-Assisted Exfoliated WS <sub>2</sub> Nanodots for Hydrogen Evolution. ACS Nano, 2016, 10, 2159-2166.	7.3	269
90	Europium Luminescence Used for Logic Gate and lons Sensing with Enoxacin As the Antenna. Analytical Chemistry, 2016, 88, 1238-1245.	3.2	42

#	Article	IF	CITATIONS
91	Cobalt disulfide nanowires as an effective fluorescent sensing platform for DNA detection. Journal of Materials Chemistry B, 2016, 4, 2860-2863.	2.9	15
92	In Situ Electrochemically Activated CoMn-S@NiO/CC Nanosheets Array for Enhanced Hydrogen Evolution. ACS Catalysis, 2016, 6, 2797-2801.	5.5	99
93	A dual-mode signaling response of a AuNP-fluorescein based probe for specific detection of thiourea. Analyst, The, 2016, 141, 2581-2587.	1.7	40
94	Fluorescent and Colorimetric Dual-Readout Assay for Inorganic Pyrophosphatase with Cu <sup>2+</sup> -Triggered Oxidation of <i>o</i> -Phenylenediamine. Analytical Chemistry, 2016, 88, 1355-1361.	3.2	140
95	An anti-fouling aptasensor for detection of thrombin by dual polarization interferometry. Chemical Communications, 2015, 51, 5645-5648.	2.2	18
96	Gold nanoclusters–Cu2+ ensemble-based fluorescence turn-on and real-time assay for acetylcholinesterase activity and inhibitor screening. Biosensors and Bioelectronics, 2015, 74, 177-182.	5.3	68
97	Integrated Logic Gate for Fluorescence Turn-on Detection of Histidine and Cysteine Based on Ag/Au Bimetallic Nanoclusters–Cu2+Ensemble. ACS Applied Materials & Interfaces, 2015, 7, 6860-6866.	4.0	90
98	A dual-mode colorimetric and fluorometric "light on―sensor for thiocyanate based on fluorescent carbon dots and unmodified gold nanoparticles. Analyst, The, 2015, 140, 8157-8164.	1.7	68
99	A simple and sensitive assay for the determination of nitrite using folic acid as the fluorescent probe. Analytical Methods, 2015, 7, 1543-1548.	1.3	25
100	A new colorimetric protocol for selective detection of phosphate based on the inhibition of peroxidase-like activity of magnetite nanoparticles. Analytical Methods, 2015, 7, 161-167.	1.3	36
101	Highly Sensitive Real-Time Assay of Inorganic Pyrophosphatase Activity Based on the Fluorescent Gold Nanoclusters. Analytical Chemistry, 2014, 86, 7883-7889.	3.2	118
102	An electrochemical sensor for dopamine based on poly(o-phenylenediamine) functionalized with electrochemically reduced graphene oxide. RSC Advances, 2014, 4, 3743-3749.	1.7	18
103	A fluorescence glucose sensor based on pH induced conformational switch of i-motif DNA. Talanta, 2014, 129, 539-544.	2.9	19
104	Real-Time Study of Interactions between Cytosine–Cytosine Pairs in DNA Oligonucleotides and Silver Ions Using Dual Polarization Interferometry. Analytical Chemistry, 2014, 86, 3849-3855.	3.2	37
105	Synthesis of graphene nanosheets with incorporated silver nanoparticles for enzymeless hydrogen peroxide detection. Analytical Methods, 2013, 5, 2298.	1.3	40
106	Microorganismâ€Derived Heteroatomâ€Doped Carbon Materials for Oxygen Reduction and Supercapacitors. Advanced Functional Materials, 2013, 23, 1305-1312.	7.8	213
107	Noble Metal Nanoparticles in Bioanalysis. ACS Symposium Series, 2012, , 241-279.	0.5	0
108	Tunable fluorescence emission of ternary nonstoichiometric Ag–In–S alloyed nanocrystals. Journal of Nanoparticle Research, 2012, 14, 1.	0.8	6

#	Article	IF	CITATIONS
109	Dual polarisation interferometry for real-time, label-free detection of interaction of mercury(ii) with mercury-specific oligonucleotides. Chemical Communications, 2012, 48, 2873.	2.2	25
110	Sulfite recognition and sensing using Au nanoparticles as colorimetric probe: a judicious combination between anionic binding sites and plasmonic nanoparticles. Analytical Methods, 2012, 4, 1616.	1.3	13
111	Probing Biomolecular Interactions with Dual Polarization Interferometry: Real-Time and Label-Free Coralyne Detection by Use of Homoadenine DNA Oligonucleotide. Analytical Chemistry, 2012, 84, 924-930.	3.2	26
112	Preparation of the 12-Molybdophosphoric Acid-Layered Double Hydroxides Nanocomposite Hybrid and its Electrocatalytic Reduction of Halate Ions. Analytical Letters, 2012, 45, 1910-1918.	1.0	1
113	Capillary Electrophoresis Coupled with Electrochemiluminescence for the Facile Separation and Determination of Salbutamol and Clenbuterol in Urine. Electroanalysis, 2012, 24, 1597-1603.	1.5	20
114	Colorimetric logic gates for small molecules using split/integrated aptamers and unmodified gold nanoparticles. Chemical Communications, 2011, 47, 9435.	2.2	67
115	Facile colorimetric detection of glucose based on an organic Fenton reaction. Analytical Methods, 2011, 3, 1056.	1.3	13
116	Sensitive electrochemical sensor for hydrogen peroxide using Fe3O4 magnetic nanoparticles as a mimic for peroxidase. Mikrochimica Acta, 2011, 174, 183-189.	2.5	50
117	Polymer wrapping technique: an effective route to prepare Pt nanoflower/carbon nanotube hybrids and application in oxygenreduction. Energy and Environmental Science, 2010, 3, 144-149.	15.6	45
118	Spectrophotometric detection of lead(II) ion using unimolecular peroxidase-like deoxyribozyme. Mikrochimica Acta, 2010, 171, 195-201.	2.5	40
119	Electrochemiluminescence Enhancement of CdTe Quantum Dots by the Addition of Silver(I) Ions. Analytical Letters, 2010, 43, 2837-2847.	1.0	7
120	Optical Extinction Combined with Phase Measurements for Probing DNAâ^'Small-Molecule Interactions Using an Evanescent Waveguide Biosensor. Analytical Chemistry, 2010, 82, 5455-5462.	3.2	16
121	Real-Time Study of Genomic DNA Structural Changes upon Interaction with Small Molecules Using Dual-Polarization Interferometry. Analytical Chemistry, 2009, 81, 4914-4921.	3.2	31
122	Kinetic analysis of interaction between lipopolysaccharide and biomolecules. Frontiers of Chemistry in China: Selected Publications From Chinese Universities, 2008, 3, 14-17.	0.4	3
123	Interaction between bovine serum albumin and Indo-1 using fluorescence spectroscopic method. Frontiers of Chemistry in China: Selected Publications From Chinese Universities, 2008, 3, 105-111.	0.4	8
124	Determination of benzhexol and procyclidine using an electrochemiluminescence-based sensor constructed by a screen-print technique. Mikrochimica Acta, 2008, 162, 211-217.	2.5	11
125	A Simple and Inexpensive Method for Fabrication of Ultramicroelectrode Array and Its Application for the Detection of Dissolved Oxygen. Electroanalysis, 2008, 20, 797-802.	1.5	11
126	Template-Free, Surfactantless Route to Fabricate In(OH) <sub>3</sub> Monocrystalline Nanoarchitectures and Their Conversion to In <sub>2</sub> O <sub>3</sub> . Crystal Growth and Design, 2008, 8, 950-956.	1.4	91

#	Article	IF	CITATIONS
127	Electrochemical Detection of Anions on an Electrophoresis Microchip with Integrated Silver Electrode. Electroanalysis, 2005, 17, 1222-1226.	1.5	10
128	Immobilization of Glycosylated Enzymes on Carbon Electrodes, and its Application in Biosensors. Mikrochimica Acta, 2005, 150, 21-26.	2.5	10
129	Capillary Electrophoresis with Indirect Electrochemiluminescence Detection. Analytical Letters, 2005, 38, 1179-1191.	1.0	12
130	Mimetic Membrane for Biosensors. Analytical Letters, 2005, 38, 3-18.	1.0	10
131	Electropolymerization of Azure B on a Screen-Printed Carbon Electrode and its Application to the Determination of NADH in a Flow Injection Analysis System. Mikrochimica Acta, 2004, 148, 335-341.	2.5	38
132	The Modification of Screen-Printed Carbon Electrodes with Amino Group and Its Application to Construct a H2O2 Biosensor. Electroanalysis, 2004, 16, 730-735.	1.5	16
133	Determination of Reserpine in Urine by Capillary Electrophoresis with Electrochemiluminescence Detection. Electroanalysis, 2004, 16, 169-174.	1.5	39
134	Characterization of organic–inorganic multilayer films by cyclic voltammetry, UV–Vis spectrometry, X-ray photoelectron spectroscopy, small-angle X-ray diffraction and electrochemical impedance spectroscopy. Journal of Materials Chemistry, 2002, 12, 1724-1729.	6.7	7
135	Simultaneous Determination of Tramadol and Lidocaine in Urine by End-column Capillary Electrophoresis with Electrochemiluminescence Detection. Electroanalysis, 2002, 14, 1571-1576.	1.5	63
136	Assembly of Alternating Polycation and DNA Multilayer Films by Electrostatic Layer-by-Layer Adsorption. Biomacromolecules, 2001, 2, 463-468.	2.6	127
137	Enhanced surface plasmon resonance immunosensing using a streptavidin–biotinylated protein complex. Analyst, The, 2001, 126, 4-6.	1.7	29
138	Methods to study the ionic conductivity of polymeric electrolytes using a.c. impedance spectroscopy. Journal of Solid State Electrochemistry, 2001, 6, 8-15.	1.2	119
139	A New Kind of Potassium Sensor Based on Capacitance Measurement of Mimic Membrane. Electroanalysis, 2001, 13, 68-71.	1.5	14
140	Formation and Characterization of Heteropolyacid/Polycation Multilayer Films on Gold Electrode. Journal of the Electrochemical Society, 2001, 148, E227.	1.3	16
141	Determination of Propranolol by Capillary Electrophoresis with End-Column Amperometric Detection. Electroanalysis, 2000, 12, 535-537.	1.5	14
142	Simultaneous Determination of 2-Aminothiazole, 2-Aminobenzothiazole and 2-Mercaptobenzothiazole by Capillary Electrophoresis with End-Column Amperometric Detection. Electroanalysis, 2000, 12, 821-824.	1.5	1
143	Determination of Three $\hat{l}^2$ -Blockers by Capillary Electrophoresis with End-Column Electrochemical Detection. Electroanalysis, 2000, 12, 1379-1382.	1.5	14
144	Ion Channel Behavior of Supported Bilayer Lipid Membranes on a Glassy Carbon Electrode. Analytical Chemistry, 2000, 72, 6030-6033.	3.2	57

2

#	Article	IF	CITATIONS
145	Determination of Surface pKa of SAM Using an Electrochemical Titration Method. Electroanalysis, 1999, 11, 1108-1113.	1.5	143

146 Determination of Surface pKa of SAM Using an Electrochemical Titration Method. , 1999, 11, 1108.